

Characterization by a time-frequency method of classical waves propagation in one-dimensional lattice : effects of the dispersion and localized nonlinearities.

O. Richoux, C. Depollier, J. Hardy

July 10, 2009

PACS : 43.60.Qv, 43.20.Mv, 43.25.Zx.

Abstract

This paper presents an application of time-frequency methods to characterize the dispersion of acoustic waves travelling in a one-dimensional periodic or disordered lattice made up of Helmholtz resonators connected to a cylindrical tube. These methods allow (1) to evaluate the velocity of the wave energy when the input signal is an acoustic pulse ; (2) to display the evolution of the spectral content of the transient signal ; (3) to show the role of the localized nonlinearities on the propagation *.i.e* the emergence of higher harmonics. The main result of this paper is that the time-frequency methods point out how the nonlinearities break the localization of the waves and/or the filter effects of the lattice.

1 Introduction

When considering propagation of acoustical pulses in dispersive media, the crucial question is that of the spreading of the signals. Indeed, the investigation of the dispersion relation gives a lot of information about the processes which play a part in the wave propagation. Efficient tools for characterizing the temporal localization of the spectral components are the Time-Frequency Representations (TFR) of signals. Joint time-frequency representations combine time and frequency-domain analysis by displaying a

signal as a function defined over the time frequency plane. These representations make the behavior of transient signal visible which is, if not impossible, at least, very difficult by using harmonic analysis. For waves travelling in strongly dispersive media (*e.g.* a periodic lattice) these approaches can be very useful since they allow the determination of the dispersion relations by measurement of the time of arrival of the different components (or frequencies) of the input signal. When the propagating medium contains nonlinearities, the TFR lead also to a detailed visualization of the nonlinear effects and show their consequences for the propagation of signals.

In the following, the dispersion characteristics of sound waves propagating in a waveguide with an array of Helmholtz resonators connected axially are examined. From a general model of propagation taking account of weakly nonlinear effects localized in the resonators, we present Time-Frequency pictures given by acoustic pulses and frequency modulated signals (chirps).

2 Propagation in a one-dimensional discrete medium

2.1 Lattice description

A one-dimensional lattice made up of an infinitely long cylindrical waveguide (call also pipe) connected to an array of Helmholtz resonators numbered by n (simply call resonator hereafter) is considered. The

resonators are connected to the pipe through a pin-point connection, the radius of the throat's cross sectional area s_n of the n^{th} resonator being assumed to be small compared to the wave length of the acoustic wave ($\sqrt{s_n}/\lambda \ll 1$). Each connection is located along the axis of the waveguide by its coordinate z_n with axial spacing d_n for two consecutive points as shown in Fig. (1).

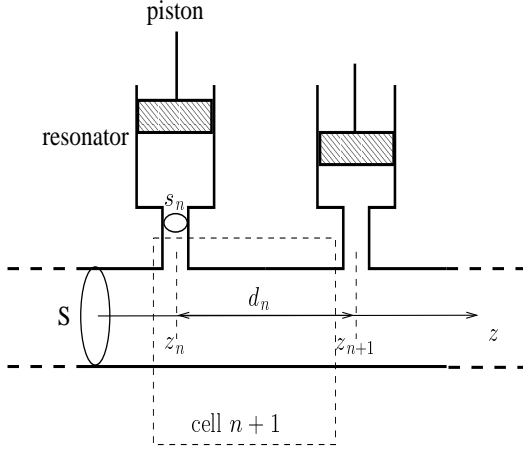


Figure 1: Experimental set up.

2.2 General case

In a section of the pipe between two consecutive connection points, the acoustic wave described by the pressure $p(z, t)$ and the acoustic velocity $v(z, t)$ is the solution of the wave equation :

$$\frac{\partial^2 p(z, t)}{\partial z^2} - \frac{1}{c^2} \frac{\partial^2 p(z, t)}{\partial t^2} = 0 \quad (1)$$

where c is the sound speed in free space.

At each connection point (Fig. (1)), the boundary conditions require the conservation of acoustic flow and continuity of acoustic pressure :

$$v(z, t)|_{z_n^+} - v(z, t)|_{z_n^-} = -\frac{s_n}{S} v_t(z_n, t) \quad (2)$$

$$p(z, t)|_{z_n^+} = p(z, t)|_{z_n^-} \quad (3)$$

where $v_t(z_n, t)$ is the acoustic velocity in the throat of the $(n+1)^{\text{th}}$ resonator. By using the Euler equation,

Eq. (2) and (3) become

$$\left. \frac{\partial p(z, t)}{\partial x} \right|_{z_n^+} - \left. \frac{\partial p(z, t)}{\partial x} \right|_{z_n^-} = -\frac{\rho s_n}{S} \frac{\partial v_t(z_n, t)}{\partial t} \quad (4)$$

$$p(z, t)|_{z_n^+} = p(z, t)|_{z_n^-} \quad (5)$$

where ρ is the air density. They lead to the inhomogeneous wave equation [1] :

$$\frac{\partial^2 p(z, t)}{\partial z^2} - \frac{1}{c^2} \frac{\partial^2 p(z, t)}{\partial t^2} = \sum_n \delta(z - z_n) \frac{-\rho s_n}{S} \frac{\partial v_t(z, t)}{\partial t}, \quad (6)$$

where the right hand side term has a comb-like structure, the teeth of which having a length related to the corresponding impedance jump. This forcing term acts as an array of secondary point-sources (scatterers) which work when they are illuminated by the wave travelling in the pipe.

2.3 Propagation of a monochromatic wave

2.3.1 Propagation equation

For a monochromatic acoustic wave with a frequency below the cut-off frequency of the waveguide, the acoustic pressure $p(z, t)$ and velocity $v(z, t)$ along the waveguide are :

$$p(z, t) = p(z) e^{j\omega t} \quad \text{and} \quad v(z, t) = v(z) e^{j\omega t},$$

where $\omega = kc$ is the angular frequency. The amplitudes $p(z)$ and $v(z)$ are related by an impedance relation. At each connection between the waveguide and a resonator, the wave impedance (which is modified by a change of cross sectional shape), the acoustic velocity and therefore the derivative of the pressure dp/dz , are discontinuous functions. Using the Eq. (6), the pressure $p(z)$ is given by the solution of the following equation :

$$\frac{d^2 p(z)}{dz^2} + k^2 p(z) = \sum_n \delta(z - z_n) \sigma_n p(z), \quad (7)$$

where $\sigma_n = -j\omega \rho s_n / (SZ_n)$. In this relation Z_n is the impedance of the n^{th} resonator connected at point

$z = z_n$ seen from the guide and σ_n is the jump of the pressure derivative $\frac{\partial p}{\partial z}|_{z=z_n}$.

2.3.2 Matrix method

In the $n + 1^{\text{th}}$ cell ($z_n \leq z < z_{n+1}$) the pressure and the acoustic velocity are respectively denoted by p_n and v_n . The solution of the Eq. (7) can be found by the matrix method [1, 2, 3] and the solution $p_n(z)$ is given as a linear combination of waves travelling in opposite direction :

$$p_n(z) = A_n e^{jk(z-z_n)} + B_n e^{-jk(z-z_n)}. \quad (8)$$

Here the coefficients A_n and B_n are respectively the amplitudes of the forward and backward waves.

This function is connected to p_{n+1} in the next region having passed through the impedance discontinuity at the connection point z_n . The connectivity conditions at the scattering region are the continuity of the pressure

$$p_n(z_n) = p_{n+1}(z_n),$$

and the continuity of the mass flux

$$\frac{1}{p_{n+1}(z)} \frac{\partial p_{n+1}(z)}{\partial z} \Big|_{z=z_n^+} - \frac{1}{p_n(z)} \frac{\partial p_n(z)}{\partial z} \Big|_{z=z_n^-} = \sigma_n.$$

These junction conditions ensure a physically sound solution by requiring continuity all along the waveguide. Applying the matrix method, these equations may be reduced to a transfer matrix \mathcal{D}_n relating the amplitudes of waves across the junction z_n . From $z_n + \varepsilon$ to $z_{n+1} - \varepsilon$, the propagation is modeled by a phase matrix \mathcal{M}_{n+1}

$$\mathcal{M}_{n+1} = \begin{pmatrix} e^{jk(z_{n+1}-z_n)} & 0 \\ 0 & e^{-jk(z_{n+1}-z_n)} \end{pmatrix}.$$

The transfer matrix of propagation over the region $z_n \leq z < z_{n+1}$ is $\mathcal{T}_{n+1} = \mathcal{M}_{n+1} \mathcal{D}_n$. In this way the pressure in the duct is given by the following recursive relation :

$$V_{n+1} = \mathcal{T}_{n+1} V_n \quad \text{where} \quad V_n = \begin{pmatrix} A_n \\ B_n \end{pmatrix} \quad (9)$$

which links the vector pairs $(A_n B_n)^t$ and $(A_{n+1} B_{n+1})^t$. The matrix \mathcal{T}_{n+1} has the following form [1]

$$\mathcal{T}_n = \begin{pmatrix} (1 + \frac{\sigma_n}{2jk}) e^{jk d_n} & \frac{\sigma_n}{2jk} e^{-jk d_n} \\ -\frac{\sigma_n}{2jk} e^{jk d_n} & (1 - \frac{\sigma_n}{2jk}) e^{-jk d_n} \end{pmatrix}. \quad (10)$$

The propagation through the lattice from z_n to z_{n+m} is then described by the relation

$$V_{n+m} = \prod_{i=1}^m \mathcal{T}_{n+i} V_n. \quad (11)$$

V_n may be interpreted as the vector of the initial conditions (or boundary conditions) and V_{n+m} is the vector of the wave amplitudes m cells further along. The effect of disorder is always to break some symmetry [4]. In the case of our lattice disorder breaks the periodicity. So it is easier to characterize disordered systems in terms of their deviations from an ideal of order than it is to define a perfectly disordered system on which some partial degree of order is to be imposed, and, to think about a disordered system it is necessary to keep in mind the ideal system from which it derives. So, before tackling the problem of wave propagation in disordered media, some specific results about periodic lattices are recalled.

2.3.3 Periodic lattice

For an ordered (*i.e.* periodic) lattice, the transfer matrix $\mathcal{T}_n = \mathcal{T}$ is the same for every cell, and the infinite medium problem is analogous to the Krönig-Penney model well known in solid state physics to investigate the motion of electrons in a periodic potential [2]. So the propagation in the lattice can be seen in terms of plane waves subject to multiple reflections at each derivation, resulting in standing waves. It is also possible to describe the propagation in terms of a collective excitation that propagates in the periodic lattice without scattering but with a modified dispersion relation. The result is that spatial periodicity gives rise to dispersion even in the model of plane waves and in this special case the spectrum shows frequency intervals (gaps) where no energy propagates.

Studying the spectral properties of such a system is then to seek stationary states of excitation that satisfy prescribed conditions at one end of the lattice.

The general theory of eigenvalues assures that the spectrum is not significantly affected by the values chosen as boundary conditions, provided the number of cells is large. The matrix \mathcal{T} has two eigenvalues α^\pm with two eigenvectors \mathbf{W}^\pm respectively. Any acoustic wave in the duct can be represented as a linear combination of these eigenvectors

$$p_n = u^+ \mathbf{W}^+ + u^- \mathbf{W}^-.$$

The effect of operating on p_n by the transfer matrix \mathcal{T} depends on the nature *i.e.* real or complex of the eigenvalues α^\pm . When they are real, \mathcal{T} simply "pushes the wave" in the direction of the eigenvector corresponding to the greatest eigenvalue. If $\alpha^+ > \alpha^-$ then

$$p_{n+m} = \mathcal{T}^m p_n \approx (\alpha^+)^m u^+ \mathbf{W}^+$$

as m becomes large. \mathbf{W}^+ is a fixed point or an invariant point of the transformation $p_{n+1} = f(p_n)$. By iteration of this transformation, \mathbf{W}^+ appears as an attractor (or a sink) in the subspace spanned the eigenvectors : almost all the waves are attracted by \mathbf{W}^+ . When the eigenvalues are complex, the iteration produces a periodic sequence : \mathbf{W}^\pm are indifferent points of the plane.

Because the transfer matrix is unitary, the eigenvalues of matrix \mathcal{T} obey to the equation

$$\alpha^2 + \alpha \text{Tr}(\mathcal{T}) + 1 = 0, \quad (12)$$

where

$$\text{Tr}(\mathcal{T}) = 2 \cos(kd) + \frac{\sigma}{k} \sin(kd) = 2 \cos(qd) \quad (13)$$

represents the dispersion relation of the Bloch waves [5], q being the Bloch wave number. This derived dispersion relation exhibits the peculiar characteristic of filters marked by forbidden frequencies or gaps or stopbands and allowed frequencies or passbands in the frequency domain which results from the resonances and the periodic arrangements of the medium. Waves that obey the relation $|\cos(qd)| \leq 1$ are within a passband and travel freely in the duct and waves such that $|\cos(qd)| > 1$ are in a forbidden band and are quickly damped spatially. They become evanescent so that they cannot propagate.

To deduce the particularity of the band structure, Eq. (13) is written in the following form

$$\cos(qd) = \frac{\cos(kd + \theta)}{\cos(\theta)}$$

where θ is defined by $\tan(\theta) = \frac{-\sigma}{2k}$. The frequencies which bound stopbands and passbands are given by the equation :

$$\cos(kd + \theta) = \pm \cos(\theta)$$

leading to two kinds of solutions $kd = n\pi$ and $kd = n\pi - 2\theta$ with $n \in \mathbb{N}$.

Two kinds of stopbands appear in the band structure : one kind called Bragg stopband due to the periodicity of the lattice, the other due to the resonances of the scatters and called resonance stopbands. A plot of the dispersion relation (13) corresponding to the ordered lattice of Helmholtz resonators is showed in Fig. 2 which illustrates the different stopbands.

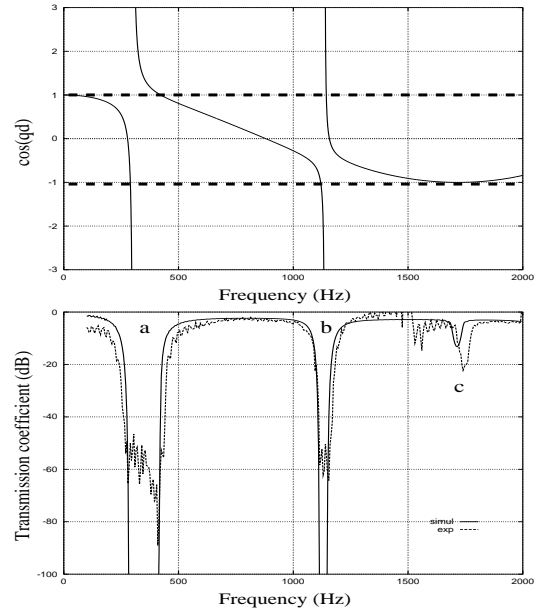


Figure 2: (a) Dispersion relation (from eq. 13) of a ordered lattice. (b) Transmission coefficient of the lattice : — simulation (from eq. 15), -- experiment.

2.3.4 The case of a disordered medium

A disordered lattice is mathematically characterized by a random sequence of non-identical transfer matrices \mathcal{T}_n whose overall product describes the propagation along the guide. The disordered linear system gives rise to the classical Anderson localization [6]. In this case, all the matrices are different each corresponding to a different cell, and the wave propagation is described by the general Eq. (11). The estimation of the Lyapunov exponent, from the Ossedec theorem [7], gives the behavior of the solution $p(z)$ in the limit $n \rightarrow +\infty$:

$$\xi = \lim_{n \rightarrow \infty} \frac{1}{n} \ln \left(\text{Tr} \left(\prod_{i=1}^n \mathcal{T}_i \right) \right). \quad (14)$$

An alternative way to analyze the behavior of the waves is the direct evaluation of $\tau_{n,m}$ defined, from Eq. (11), by

$$\tau_{n,m} = \frac{A_{n+m}}{A_n} \quad (15)$$

corresponding to the transmission coefficient of a lattice made up of m cells. As $|m| \rightarrow \infty$, $\tau_{n,m}$ is related to ξ by $\tau_{n,m} \approx \exp(-\xi|m|d)$ where d is now the mean value of the set of values $|z_i - z_{i+1}|$ *i.e.* the mean length of cells [8]. When the medium is disordered, the gaps widen : eventually waves cannot propagate in such a medium. This result is well known since Anderson's original paper [6] : in a one-dimensional disordered system, almost all the elementary excitations are localized. The waves cannot propagate in a disordered medium because of the many scatterers they encounter. The possibility that a wave can be localized in a random medium is mysterious because localization involves a change in the wave character.

2.4 Propagation in a nonlinear medium

For high sound level ($\simeq 120$ dB), the relation between the acoustic pressure and the velocity in the neck of the Helmholtz resonators is no longer linear. Nonlinearities result mainly from the complicated motion of the air near the tubes between the wave guide and the neck (throat) of the resonators and at the aperture of each resonator [9].

Consequently, Eq. (6) is a nonlinear wave equation where $v_t(z, t)$ is not a linear function of $p(z, t)$. Nevertheless we assume that the propagation (between two resonators) remains linear. So the pressure in the main pipe is calculated in the same way as for a disordered medium but now nonlinear operators describe the scattering of waves at each connection point of the lattice. A simple model of nonlinear Helmholtz resonator is developed in the following by using a Taylor's development of the restoring force due to the change of pressure in the Helmholtz cavity.

3 A simple nonlinear Helmholtz resonator model

It is well known that a simple model of the Helmholtz resonator requires the following assumptions : (1) the pressure inside the cavity is spatially uniform, (2) the fluid in the neck moves like a solid piston. In this case, the air enclosed in the resonator acts as a spring for the lumped mass of air moving within the neck. A general description of the nonlinear behavior of the Helmholtz resonator may be derived by taking into account the quadratic term in the restoring force of the spring. For thermodynamical processes that occur in the air within the cavity, the adiabatic changes of the pressure p and the volume V are related by $p_0/p = (V/V_0)^\gamma$ where the subscript 0 stands for the unperturbed reference values and γ is the specific heat ratio. The relative change of the pressure p_n in the cavity of the n^{th} resonator due to a small displacement x_n of the air in the neck induces a restoring force F_n that has the following form [10] :

$$F_n = p_n s_n = -\frac{\rho c^2 s_n^2}{V_0} [x_n - \alpha_n x_n^2 + o(x_n^3)].$$

In this equation $\alpha_n = (\gamma + 1)s_n/(2V_0)$ and c is the sound velocity given by $c = \sqrt{\gamma p_0/\rho}$. The spring force is no longer linear and its stiffness is now described by two constants. For a monochromatic wave the displacement x_n of the air in the neck is related with the acoustic velocity $v_n = v(z_n)$ by the relation $v_n = j\omega x_n$ and the Euler relation applied to the air

mass $m = \rho l'_c s_n$ (where l'_c is effective neck length) submitted to the harmonic force $p_n/(\rho l'_c) e^{j\omega t}$ gives :

$$j\omega v_n + \omega_0^2 \left[\frac{v_n}{j\omega} - \alpha_n \left(\frac{v_n}{j\omega} \right)^2 + o(v_n^3) \right] = \frac{p_n}{\rho l'_c}$$

where $\omega_0^2 = s_n c^2 / (V_0 l'_c)$ is the resonance frequency of the Helmholtz resonator. The nonlinear relation between the acoustic pressure and the velocity just outside of the opening of the n^{th} resonator is

$$p_n = Z_n^{NL} v_n.$$

Here Z_n^{NL} is the "nonlinear impedance" of the n^{th} resonator :

$$Z_n^{NL} = Z_n^L + \alpha_n \rho l'_c \frac{\omega_0^2}{\omega^2} \frac{p_n}{Z_n^L} + o\left(\left(\frac{p_n}{Z_n^L}\right)^2\right),$$

and Z_n^L is the linear impedance of the n^{th} resonator ($Z_n^L = j\omega \rho l'_c (1 - \frac{\omega_0^2}{\omega^2})$). So, the nonlinear effects lead merely to a additive correction to the linear impedance of the Helmholtz resonator which is non-vanishing only around the Helmholtz resonance ω_0 . Others nonlinear phenomenon can occur due to the presence of turbulences (vortex) which are generated around the edges of the neck [9]. According to the shape (sharp or rounded) of these edges, the physical phenomena lead to nonlinear terms more or less important [11].

4 Signal analysis

Time-frequency representations have several advantages over conventional harmonic Fourier analysis. Among these one can cite their ability to analyze multicomponent signals *i.e.* broadband signals and also signals containing several modes which interfere or combine each other. But the most important advantage is their capacity to track the time evolution of transient signals. This is exemplified by the visualization of reflected signals due to scattering waves and of the spreading of acoustic pulses in the joint time frequency plane. In this paper the quadratic TFR (QTFR) are used to determine empirically the dispersion of the waves since this provides a direct access to

the group velocity and allows to extract pertinent information associated with the waves travelling in the lattice. Unfortunately, QTFR also have some drawbacks. As it is bilinear in the signal, the QTFR of the sum of two signals is not the sum of the QTFR of each of them but has an additional cross term which gives rise to artefacts and confuses the picture in the time-frequency plane. Several solutions are available for reducing these terms, for example, by using an appropriate smoothing window function and/or the analytic signal.

For the complex-valued time signal $x(t)$, the general form of the QTFR is [12]

$$W_x(t, \omega) = \frac{1}{2\pi} \int \int \int e^{-j\vartheta t - j\tau\omega - j\vartheta u} \phi(\vartheta, \tau) x\left(t + \frac{\tau}{2}\right) x^*\left(t - \frac{\tau}{2}\right) d\tau du d\vartheta \quad (16)$$

where $\phi(\vartheta, \tau)$ is the kernel of the QTFR, * stands for complex conjugate and t and ω are time and frequency respectively. The most popular QTFR is the Wigner-Ville distribution [13] for which the kernel is $\phi(\vartheta, \tau) = 1$:

$$W_z(t, f) = \int_{-\infty}^{+\infty} z\left(t + \frac{\tau}{2}\right) z^*\left(t - \frac{\tau}{2}\right) e^{-2j\pi f\tau} d\tau. \quad (17)$$

To reduce the artefacts arising from the cross terms between the different components of the signal, we use the analytic signal [14] $z(t)$ defined by

$$z(t) = x(t) + jH[x(t)] \quad (18)$$

where $H[x(t)] = \frac{1}{\pi t} \star x(t)$ is the Hilbert transform of $x(t)$ designed by the Kaiser window method (FIR Hilbert transformer) [15]. The Pseudo Wigner-Ville distribution is given by

$$PW_z(t, f) = \int_{-\infty}^{+\infty} |h(\tau)|^2 z\left(t + \frac{\tau}{2}\right) z^*\left(t - \frac{\tau}{2}\right) e^{-2j\pi f\tau} d\tau \quad (19)$$

where $h(\tau)$ is a smoothing window (in our case a Kaiser function).

5 Experimental results

5.1 Experimental apparatus

Figure 1 shows the experimental setup. It consists of a 8 m long cylindrical pipe having a 5 cm inner diameter and a 0.5 cm thick wall connecting with an array of 60 Helmholtz resonators as side branches. The distance between two consecutive resonators is $d_n = 0.1$ m. The upstream section links this system to a loudspeaker designed for high acoustic power level and used to generate linear frequency modulated waves (chirps) or wavepackets (approximate δ -function). The duration of the chirp is 0.5 s and the frequency range is included in [100; 600] Hz. The wavepackets duration is 0.01 s and its frequency range extends from 0 to 2500 Hz. At the end of the downstream section, an approximately anechoic termination made of plastic foam suppresses reflected waves. As noted above, the QTFRs are able to discriminate the reflected signal from the incident one and an anechoic termination seems unnecessary. However, its use prevents a too heavy contamination of the useful picture in the time-frequency plane by unessential signals and thus improves the accuracy of the QTFR. Lastly, two microphones m_1 and m_2 (B&K 4136 with Nexus 2690 amplifier) measure the pressure in up and downstream sections. These microphones produce 0.2 % of distortion at 150 dB which ensures that the nonlinear effects are generated by the propagation under the lattice (and not by the microphones themselves). The data acquisition is carried out by means of a 16 bits AD-converted with a sampling frequency of 10 kHz and an anti-aliasing filter (8th order Chebyshev filter) with a bandwidth of 4 kHz.

All the resonators are identical and are $L = 16.5$ cm long cylindrical cavities with a diameter of 4 cm. Their volumes may be independently tuned by moving pistons. Their neck is a 2 cm long tube having a diameter of 1 cm. The Helmholtz resonance frequency corresponding to the whole volume ($V_0 = 2.1 \cdot 10^{-4}$ m³) is 300 Hz. All the pipes used are sufficiently stiff that their structural modes are not in the frequency range of interest.

5.2 Linear case

Figure 2 gives the theoretical $[f, \cos(qd)]$ plot of the dispersion relation of Bloch waves for the ordered lattice described above (Fig. 2-a) and the experimental results deduced from the transfer function of the system (Fig. 2-b). We observe a good fit in the frequency range of interest. For this geometry the curve shows two kinds of gaps : those (labeled a and b) due to the resonators included in [300 : 450] Hz (Helmholtz resonance) and [1100 : 1200] Hz (corresponding to the length of the cavity L) and one other that is a specific characteristic of the periodic lattice ($d_n = 0.1$ m) at 1700 Hz (labeled c). The Pseudo Wigner-Ville Distribution images associated with the propagation of an acoustic pulse in the lattice are presented in Fig. 3. Figure 3-a is the PWVD of the signal picked-up in the upstream section of the apparatus by microphone m_1 corresponding to the incident impulse beginning at 0.4 s and three narrow bands reflected signal. Fig. 3-b shows the PWVD of the transmitted (output) signal given by microphone m_2 (no reflection are visible because of the anechoic termination). As well as the time frequency plot of the incident impulse, other details can be seen in Fig. 3-a. For time $t > 0.47$ s a part of the input signal is reflected corresponding to the upper cutoff frequencies of the gaps. The two lower stopbands correspond to the energy of acoustic waves reflected by the resonators.

The third case has a different nature since this gap is due to the spatial periodicity of the lattice. The reflected signal corresponding to this stopband indicates that at least for a finite length lattice, the spectrum structure (gaps and allowed bands) is not produced only by wave interferences but also by some wave reflection. This result cannot be displayed by a method other than QTFRs since it requires time and frequency to be localized. Some authors have investigated analytically [3] or experimentally [16] the dispersion characteristics of sound waves in a lattice of Helmholtz resonators but they have not pointed out the existence of a reflected wave for particular bands.

In Fig. 3-b, the waves belonging to the allowed bands are shown at the time 0.49 s corresponding to the

propagation of waves through the lattice. The gaps are easily identified and are in good agreement with the values given by the Bloch theory. The waves with frequencies closed to the gaps arrive at longer and longer delays : their group velocity goes to zero as the frequency gets closer to the cutoff frequencies. This is indicated on the PWVD plot by long tails on each side of the gaps. From the point coordinates of PWVD of the output signal, it is possible to estimate the group velocity as a frequency dependant function (Fig. 4).

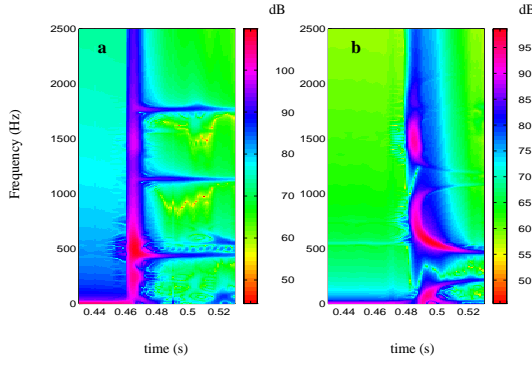


Figure 3: (a) Wigner-Ville transform of a pulse signal upstream of the lattice. (b) Wigner-Ville transform of pulse signal downstream of the lattice.

5.3 Nonlinear case

In the nonlinear case, the physical parameters of the output are dependent on the input parameters. It is then necessary to consider several cases with different input conditions. To investigate the effects of these nonlinearities, the input signal is a linear FM signal with a frequency range including the first stopband of the lattice (from 100 Hz to 600 Hz). Fig. 5 and Fig. 6 show the PWVD of this chirp for low and high acoustic levels corresponding to the linear and the nonlinear cases respectively. In the linear case, waves belonging to the first forbidden band cannot propagate, as shown by Fig. 5-b. For higher acoustic levels, nonlinearities generate harmonics 2ω and 3ω which belong to allowed bands (Fig. (7) which represents a zoom in the time scale range $[0.2s : 0.4s]$ of the

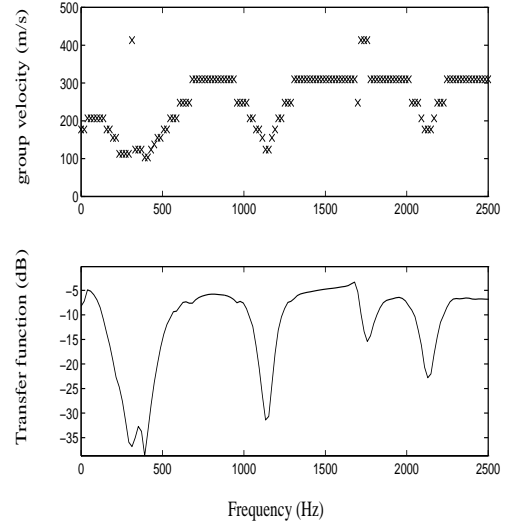


Figure 4: Group velocity vs. frequency and transfer function of the lattice.

Fig. (6)). Then, for some particular frequencies in the first stopband the nonlinearities take part to the delocalization of the energy and gives rise to energy transport : the energy of an input signal contained in a frequency range which is in a gap propagates in the lattice after being transferred in ranges corresponding to allowed bands in the spectrum. This mechanism breaks the filter structure of the lattice and is partly responsible for changes in the transmissivity of the medium. Indeed, the amplitude is restored with presence of nonlinearity : each site exhibits a nonlinearity and for localization lengths of the order of the lattice spacing, the associated wave becomes propagating. The measurement of the energy amplitude of each harmonics can permit the estimation of coefficients α_n (and the next in the Taylor's development) corresponding to the harmonics in the model developed in section 3. The Fig. (7) shows also the different phenomena induce by the nonlinear effects : in the beginning of the stopband (for time including between 0.2 and 0.25 s) only harmonic 2 is present in the response of the lattice whereas in the rest of the stopband harmonics 3, 4 and 5 are detected in the time-frequency image. Because the nonlinear ef-

fects are not the same in all the stopband, we presume that the different coefficients of the nonlinearities in the model developed in section 3 are depending on the frequency of the wave : these effects result from the competition between the different orders of the nonlinearities [17]. A experimental study of one Helmholtz resonator confirms this assumption and allows the measurement of the different coefficients of the model [18].

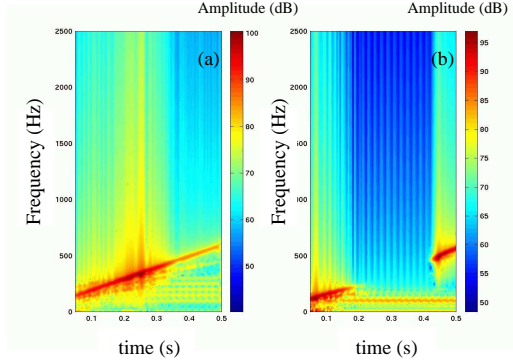


Figure 5: (a) Wigner-Ville transform of a FM signal upstream of the lattice (linear case). (b) Wigner-Ville transform of a FM signal downstream of the lattice (linear case).

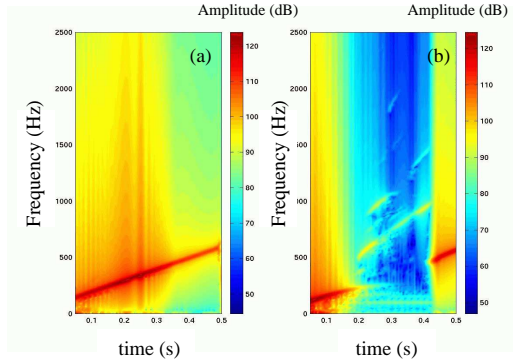


Figure 6: (a) Wigner-Ville transform of a FM signal upstream of the lattice (nonlinear case). (b) Wigner-Ville transform of a FM signal downstream of the lattice (nonlinear case).

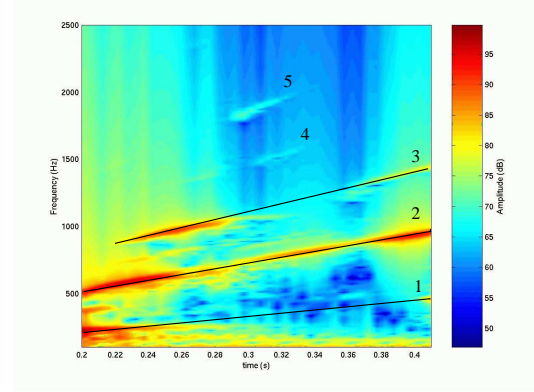


Figure 7: Zoom of the figure (6b) in the time range $[0.2 : 0.42]$ s. Numbers label the corresponding harmonics from the fundamental (1) to harmonic 5.

6 Conclusion

In this paper we have shown that the time-frequency methods are well adapted to the investigation of the propagation of dispersive waves. Especially they give information about the group velocity and allow to find the dispersion characteristics of complicated waveguide. These methods are also very efficient for displaying the nonlinear behavior of high-intensity sound waves : the generation of higher harmonics can be directly measured. Lastly, the interpretation of experimental results of wave propagation in nonlinear lattices is made easier with the help of time-frequency methods.

References

- [1] H. Levine: Unidirectional wave motion. North Holland Publisher Company, New York, 1978.
- [2] F. J. Dyson: The dynamics of a disordered linear chain. *Phys. Rev.* **92(6)** (1953) 1331–1338.
- [3] N. Sugimoto: Dispersion characteristics of sound waves in a tunnel with an array of Helmholtz resonators. *J. Acoust. Soc. Am.* **97(3)** (1994) 1446–1459.

- [4] J. M. Ziman: Models of disorder. Cambridge university press, 1978.
- [5] F. Bloch: Der quantenmechanik elektronischen. Z. Physik **55** (1928) 555.
- [6] P. W. Anderson: Absence of diffusion in certain random lattice. Phys. Rev. **109** (1958) 1492–1505.
- [7] V. I. Oseledec: A multiplicative ergodic theorem. Lyapunov characteristic numbers for dynamical systems. Trans. Moscow Math. Soc. **19** (1968) 197–230.
- [8] J. M. Luck: Systèmes désordonnés unidimensionnels. Collection Alea, Saclay, 1999.
- [9] O. V. Rudenko, K. L. Khirnykh: Helmholtz resonator model for the absorption of high-intensity sound. Sov. Phys. Acoust. **36(3)** (1990) 293–297.
- [10] R. R. Boullosa, F. O. Bustamante: The reaction force on a Helmholtz resonator driven at high sound pressure amplitudes. Am. J. Phys. **60(8)** (1992) 722–726.
- [11] S. Dequand: Duct aeroacoustics: from technological applications to the flute. Dissertation. Technische Universiteit Eindhoven TU/e and Université du Maine, 2001.
- [12] L. Cohen: Time frequency analysis. Englewood Cliffs (N. J.), Prentice Hall, 1995.
- [13] W. Mecklenbräuer, F. Hlawatsch: The Wigner distribution : Theory and applications in signal processing. editors Elsevier, Amsterdam, 1997.
- [14] D. Gabor: Theory of communication. Proc. IEEE **93(3)** (1946) 429–457.
- [15] A. V. Oppenheim, R. W. Schaffer: Discrete-time signal processing. Prentice Hall signal processing series, 1999.
- [16] C. E. Bradley: Acoustic Bloch wave propagation in a periodic waveguide. Diploma Thesis. The University of Texas, Austin, 1990.
- [17] O. Richoux, C. Depollier, G. Gonon. in preparation.
- [18] O. Richoux: Etude de la propagation des ondes mécaniques dans un réseau unidimensionnel comportant du désordre et/ou des non-linéarités localisées. Dissertation. Université du Maine, Le Mans, 1999.